ACS APPLIED MATERIALS & INTERFACES

Research Article

www.acsami.org

Ultrahigh Aspect Ratio Copper-Nanowire-Based Hybrid Transparent Conductive Electrodes with PEDOT:PSS and Reduced Graphene Oxide Exhibiting Reduced Surface Roughness and Improved Stability

Zhaozhao Zhu,*[,†] Trent Mankowski,*[,†] Kaushik Balakrishnan,[†] Ali Sehpar Shikoh,[‡] Farid Touati,[‡] Mohieddine A. Benammar,[‡] Masud Mansuripur,[†] and Charles M. Falco[†]

[†]College of Optical Sciences, The University of Arizona, 1630 East University Boulevard, Tucson, Arizona 85721, United States

[‡]Department of Electrical Engineering, College of Engineering, Qatar University, P. O. Box 2713, Doha, Qatar

Supporting Information

ABSTRACT: Copper nanowires (CuNWs) with ultrahigh aspect ratio are synthesized with a solution process and spray-coated onto select substrates to fabricate transparent conductive electrodes (TCEs). Different annealing methods are investigated and compared for effectiveness and convenience. The CuNWs are subsequently combined with the conductive polymer poly(3,4-ethylenedioxythiophene) poly(styrenesulfonate) (PEDOT:PSS) or with reduced graphene oxide (rGO) platelets in order to reduce the surface roughness and improve the durability of the fabricated TCEs. Our best-performing PEDOT:PSS/CuNW films have optical transmittance T_{550} = 84.2% (at λ = 550 nm) and sheet resistance R_s = 25 Ω/sq, while our best CuNW/rGO films have T_{550} = 84% and R_s = 21.7 Ω/sq.

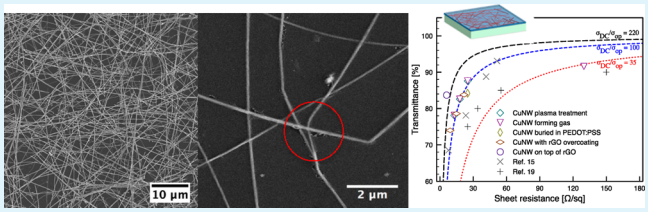

KEYWORDS: *nanowires, reduced graphene oxide, conductive polymer, hybrid thin films, transparent conductive electrodes*

1. INTRODUCTION

Transparent conductive electrodes (TCEs) are widely used in applications ranging from touch screens and displays in consumer electronics to light emitting diodes and solar panels.[1−5] Among the relevant performance characteristics, sheet resistance (R_s) and optical transmittance (T) are two key parameters commonly used to assess the suitability of a TCE for practical applications. In general, low sheet resistance and high optical transmittance are desired, although the minimum requirements vary depending on the specific application. With a typical transmittance of greater than 85% at visible wavelengths (400 nm ≤ λ ≤ 700 nm), a sheet resistance below 200 Ω/sq is usually sufficient for many touch-screen applications, while R_s ≤ 10Ω/sq is necessary for solar cells and OLEDs.

The present industry standard for TCEs is indium tin oxide (ITO), which has R_s ≈ 10 Ω/sq and T ≈ 90% for visible light.[6−8] However, due to the scarcity of indium, there has been a push toward finding alternative coating materials that can match or improve upon the performance metrics offered by ITO. Moreover, TCEs that are compatible with flexible substrates are favored nowadays for applications such as wearable electronics, a market in which ITO fails due to its rigidity. Because of these drawbacks, much effort has been directed in recent years toward finding substitute materials for ITO.

Several alternatives have been investigated during the past decade to serve as TCE. Indium-free conductive metal oxides, for instance, doped zinc oxide and tin oxide, have been the subject of many investigations. Typically, large energy input and a vacuum environment are required to produce high-quality oxide films using thin-film deposition techniques.[9] Other fabrication methods such as sol−gel deposition at high annealing temperatures have also been used to produce conductive oxide coatings.[10,11] Carbon-based nanomaterials such as carbon nanotubes and graphene have been used to fabricate TCEs as well. Carbon-nanotube-based TCEs typically have R_s = 150 Ω/sq at T ≈ 80%.[5] With a sheet resistance of 30 Ω/sq at T = 90%, continuous graphene films grown with chemical vapor deposition show excellent performance.[1] Solution-processed graphene flakes are also investigated due to their low cost and ease of fabrication; these TCEs exhibit R_s values ranging from 200 to 300 Ω/sq at T = 80%.[4] Among all the materials investigated to date, percolating metal nanowire films are the most promising choices for TCEs. Specifically, silver nanowire (AgNW) ink synthesized via a solution route can be readily deposited on select substrates using techniques such as spin-coating, spray-coating, dip-coating, Mayer-rod coating, or vacuum filtration followed by dry transfer. Each of these methods has been employed to produce high-performance TCEs.[12]

Copper has a low bulk resistivity (i.e., 16.8 nΩ·m compared to 15.9 nΩ·m for silver). Rathmell et al. have demonstrated the synthesis and deposition of copper nanowires (CuNWs) in large quantities;[13] these CuNWs can be readily deposited on

Received: February 11, 2015
Accepted: July 7, 2015
Published: July 7, 2015

DOI: 10.1021/acsami.5b01379
ACS Appl. Mater. Interfaces 2015, 7, 16223−16230

different supports using the above-mentioned methods for AgNWs. However, owing to these CuNWs' low aspect ratio, the sheet resistance and optical transmittance of the fabricated TCEs were still not suitable for many applications. According to the prediction of one-dimensional stick percolation theory,[14] the nanowire density N is related to the length of wire L in accordance with $N = ((4.236/L)^2/\pi)$. This indicates that the longer the nanowires are, the fewer of them will be needed to form a percolating network, which will then occlude less light. Knowing the importance of the length of nanowires in TCE applications, Guo et al. employed a catalytic effect to synthesize CuNWs with large aspect ratios.[15]

While CuNWs are promising materials for TCE applications, there remain many challenges that need to be addressed prior to their commercialization. Annealing of the as-produced nanowire coatings at moderate to high temperatures is necessary to form good contacts at wire−wire junctions in order to achieve acceptable levels of electrical conductivity (i.e., achieve sufficient percolation). However, the annealing temperatures are usually high enough to prevent the use of flexible substrates. In addition, copper is known to oxidize in air. The degradation due to oxidation will be far more substantial for nanowires than for bulk copper, because of the larger surface area of the nanowires that is exposed to the air. From a device integration perspective, the surface roughness of the TCEs is also a crucial limiting factor in many applications: since the percolating nanowire network contains hills at wire−wire junctions and voids in between the wires, the existence of such peaks and valleys could give rise to electrical shunts and shorts in the fabricated devices.[16]

In this work, we synthesized ultralong CuNWs using a solution method adopted from the work of Guo et al.[15] and obtained TCEs that are, in some respects, superior to those fabricated with previously synthesized copper and silver nanowires. We then adopted a transfer technique to deposit CuNWs onto a PET substrate, thus avoiding the exposure of the substrate to annealing procedures. We also managed to embed our copper nanowires in a PEDOT:PSS thin film, which helped to reduce the surface roughness of our TCEs. This aspect of our work is in fact very similar to what Gaynor et al.[16] have reported in conjunction with their silver nanowires. Additionally, by applying reduced graphene oxide (rGO) platelets as an overcoating layer to our bare CuNW films, we succeeded in preventing the oxidation of CuNWs and also improving the stability of our TCEs in high-humidity and high-temperature environments.

2. EXPERIMENTS

2.1. Nanowire Synthesis. Two methods of copper nanowire synthesis were carried out in order to compare the resulting aspect ratios. Our first method of CuNW synthesis was a one-step solution process following several procedures reported by Rathmell et al.[13] and is summarized in the Supporting Information. The nanowires were found to be between 30 and 50 μm long, with diameters ranging from 120 to 500 nm.

Our second method of CuNW synthesis followed the one-step solution process of Guo et al.[15] and is used throughout this work. Briefly, 20 mL of oleylamine was pipetted into a 50 mL capacity round-bottom three-neck flask, in which temperature was precisely controlled by a Glas-Col Digi-II system. Subsequently 1.6 mmol $CuCl_2$ and 0.8 mmol $Ni(acac)_2$ were added to the flask, which was purged with high-purity argon. The mixture was vigorously stirred and kept at 80 °C for 30 min to achieve a full dissolution that had a dark blue color. The temperature was then ramped up to 175 °C to initiate the anisotropic growth of copper nanowires. This reaction continued for at least 10 h, during which high-purity argon was purged into the flask. During the reaction, the solution underwent color changes from dark blue to clear brown to opaque red. After the reaction was completed, the red suspension was allowed to cool down to room temperature. An equal volume of hexane was poured into the flask to precipitate the nanowires from the solution. Copper nanowires were then separated from the solvent via centrifugation (6000 rpm, 15 min, at least 3 times), followed by dispersing in an isopropyl alcohol (IPA) solution containing 1 wt % poly(vinylpyrrolidone) (PVP). Finally, the nanowires were washed and stored in IPA.

2.2. Fabrication of CuNW TCEs. Several methods of TCE fabrication were used with both AgNW or CuNW combined with graphene coating, or PEDOT:PSS coating, to determine the best performers. The results obtained with silver nanowires and with the initially synthesized copper nanowires are detailed in the Supporting Information. The second method of copper nanowire growth described in the preceding subsection yielded the highest aspect-ratio nanowires (see the Results and Discussion section); the majority of our investigations involving flexible substrates and resulting in our highest performing samples were carried out using these materials. Suspensions of CuNWs in IPA form a stable solution that can be readily spray-coated via an airbrush (Paasche Model H) onto a flat substrate. Glass substrates were fixed on a tilted hot-plate, on which the temperature was maintained at 60 °C to facilitate evaporation of the solvent and to avoid flooding. The spraying condition was optimized for uniform distribution of the nanowire network, with the spraying distance of 10 cm and the spraying pressure in the delivery tube ∼15 psi. The density of nanowires can be controlled by varying the volume of material sprayed onto the target substrate. Larger volumes of sprayed CuNW suspension consistently resulted in denser networks.

To remove the excess organics and to improve contact at wire−wire junctions, two different annealing techniques were used following the spray-coating of the substrates. In one case, the samples were annealed in a tube furnace under a forming gas (95% N_2 + 5% H_2) environment at various temperatures for 1 h. Upon completion, the samples were cooled to room temperature in the forming gas atmosphere in order to avoid reoxidation. In the other case, annealing was performed using low-pressure (<5 Torr) air plasma (PLASMA-PREEN-II-862) for 2 min.

2.3. Fabrication of PEDOT:PSS/CuNW Hybrid Thin Films. PEDOT:PSS modified with 5 wt % dimethyl sulfoxide (DMSO) was used to spin-coat flexible PET substrates.[17] Prior to deposition, the PET substrates were plasma-cleaned for 20 s to improve their hydrophilicity. Typically, 0.4 mL of DMSO-modified PEDOT:PSS was pipetted onto the substrate and spun at 2000 rpm for 40 s, followed by 4000 rpm for 15 s to dry the film.

To fabricate the PEDOT:PSS hybrid films, a preannealed CuNW film on a glass substrate was placed facing down onto the PEDOT:PSS layer. The CuNW film was subsequently transferred and embedded into the PEDOT:PSS layer by applying a pressure of ∼20 MPa using a shop press. The pressure was applied for at least 10 s before lifting the upper (denuded) substrate.

2.4. Fabrication of CuNW/Reduced Graphene Oxide (rGO) Hybrid Thin Films. Graphene oxide (GO) was purchased from Graphene Supermarket. GO was separated from the stock solvent via centrifugation and dispersed in IPA at 0.02 mg/mL. The IPA suspension was spray-coated onto a CuNW film (prior to annealing the CuNWs) under the same spraying conditions as described earlier. The samples were then annealed in a forming gas (95% N_2 + 5% H_2) environment at 200 °C for 1 h.

2.5. Sample Characterization. Scanning electron microscope (SEM, Hitachi S-4800 Type II) was used to examine fabricated CuNW films, PEDOT:PSS/CuNW films, and CuNW/rGO films. Cross-sectional SEM images were captured by mounting the substrate vertically, while angled SEM images of the PEDOT:PSS/CuNW films were captured by mounting the samples vertically and tilting the stage by 5°. Atomic force microscopy (AFM) was used to study the surface morphology of synthesized materials and fabricated thin films. Raman

DOI: 10.1021/acsami.5b01379
ACS Appl. Mater. Interfaces 2015, 7, 16223−16230

spectroscopy data for GO and rGO were acquired using Renishaw's structural and chemical analyzer. Optical transmittances were measured by a Cary UV−vis−NIR spectrophotometer and corrected with blank substrates. Haze measurements were conducted with an integrating sphere, using SuperK COMPACT super continuum white light laser (450−2400 nm) and Ocean Optics USB4000 Spectrometer as detector. Sheet resistances were measured with a four-point probe (SRM-232-2000) at multiple locations on all samples. A Veeco DEKTAK 150 Profilometer was used to measure the surface profiles of the PEDOT:PSS/CuNW films.

3. RESULTS AND DISCUSSION

3.1. CuNW Synthesis. CuNWs were synthesized using the solution process suggested by Guo et al.[15] A photograph of a homogeneous CuNW suspension in IPA is shown in Figure 1a.

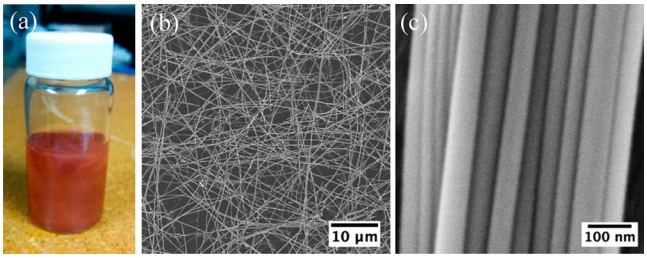

Figure 1. (a) Photograph of synthesized CuNWs in IPA suspension. (b) SEM image of synthesized CuNWs spray-coated onto a glass substrate; the nanowires are seen to be homogeneously distributed. (c) SEM image of a nanowire bundle shows the fairly uniform diameter of the wires.

Scanning electron microscopy (SEM) was conducted to study the dimensions of the synthesized nanowires, which were spray-coated (using an airbrush) onto glass substrates. A randomly oriented but uniformly distributed network of nanowires was seen to have formed after spraying; see Figure 1b. We randomly selected 50 nanowires from the SEM images and measured an average length of 75 μm and an average diameter of 45 nm, corresponding to an aspect ratio of ~1600 (see Figure 1 of the Supporting Information). A high-magnification SEM image (Figure 1c) of a nanowire bundle reveals a narrow distribution of wire diameters. Atomic force microscopy revealed the smoothness of the nanowire surfaces (see Figure 2).

Due to the insulating nature of the organic coatings that remain on nanowires after the fabrication process is completed, the wire−wire junctions typically have high electrical resistance; as a result, the samples are not electrically conductive. Removal of the organics is thus necessary to improve electrical contact at wire−wire junctions. Thermal annealing and plasma treatment of the spray-coated CuNW thin films were employed for removal of the organics and for causing the nanowires at overlapping junctions to meld. The two methods exhibited varying degrees of effectiveness and practical convenience. Thermal annealing of spray-coated CuNWs was conducted on five samples with similar nanowire densities under a forming gas (95% N_2 + 5% H_2) environment at temperatures ranging from 100 to 300 °C, in 50 °C increments for 1 h. Upon completion of the annealing process, the samples were cooled to room temperature. (It is important that the samples are cooled in the reducing atmosphere in order to avoid reoxidation.) The sheet resistance of each annealed sample was measured with a four-point probe at multiple locations and then averaged for each sample. From Figure 3a, it is seen that the sheet resistance and also the standard deviation of the measurements are optimum when the sample is annealed at 200 °C. Figures 3c and 3d are AFM images of wire−wire junctions for unannealed and annealed samples, respectively, while Figures 3e and 3f show the corresponding line-height profiles for the two samples. For the unannealed sample, the junction height (red profile) is approximately the sum of the heights of two individual wires (black profile). However, for the annealed sample, the junction height is seen to be only slightly higher than that of each individual wire, indicating nanofusion. This melding of the nanowires at various junctions is believed to be primarily responsible for improvements of the sheet resistance. As we increased the annealing temperature beyond 200 °C, the sheet resistance increased slightly, presumably due to the coalescence of CuNWs.[14]

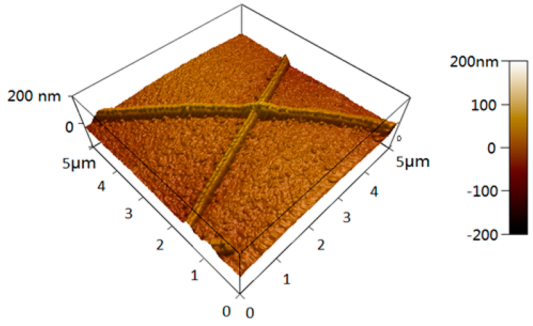

Figure 2. 3D reconstructed AFM image showing the smoothness of the nanowire surface.

Removal of organic coatings of CuNWs could also be achieved using plasma treatment (as an alternative to thermal annealing). The plasma treatment was carried out under a low-pressure air environment (<5 Torr) for 2 min, which is approximately the maximum treatment time before sample deformation occurs (see Figure 2 of the Supporting Information). Figure 3b provides a comparison of the samples in terms of their sheet resistance R_s and optical transmittance T_{550} obtained using each annealing method under its respective optimal conditions (i.e., thermal annealing at 200 °C for 1 h and plasma treatment under low-pressure air for 2 min). While thermal annealing in a forming gas atmosphere provides slightly better sheet resistance at a given optical transmittance compared to plasma treatment, the latter method has the advantages of speed (2 min compared to over an hour, including cooling) and simplicity (e.g., no need for a special gas). These features of plasma treatment will, of course, be advantageous in commercial grade fabrication.

3.2. Composite CuNW Electrode with PEDOT:PSS. It is a well-known fact that excessive surface roughness of an electrode could adversely affect its performance in many optoelectronic applications.[16,18] With our CuNW TCEs, since the nanowires form an interconnected network by stacking on top of each other, the wire−wire junctions are significantly elevated above the voids in between nanowires. This rough morphology of the nanowire network can result in local thinning of any active or passive layer that is subsequently deposited over the metallic network, which could lead to shunting or shorting.[18] In order to reduce the surface roughness of our CuNW TCEs, we adopted a transfer method similar to that reported in the pioneering work of Gaynor et al. in conjunction with their AgNW transparent electrodes.[16] Preannealed CuNW films on a glass substrate were transferred

DOI: 10.1021/acsami.5b01379
ACS Appl. Mater. Interfaces 2015, 7, 16223−16230

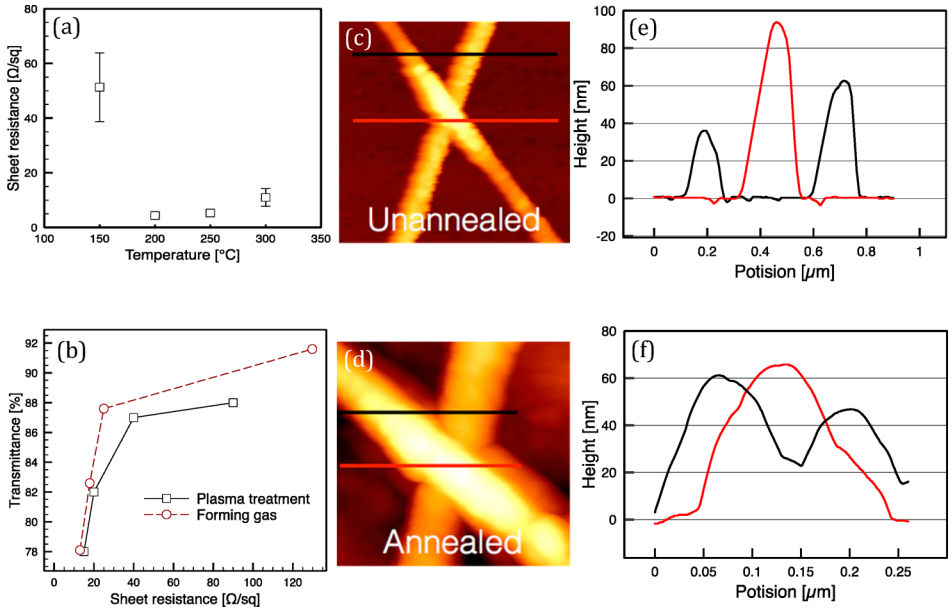

Figure 3. (a) Measured sheet resistance R_s versus annealing temperature in a forming gas atmosphere for 1 h. (b) Optical transmittance T_{550} versus sheet resistance R_s for thermal annealing in forming gas (red) and for plasma cleaning (black). (c) AFM image of an unannealed nanowire junction. (d) AFM image of an annealed nanowire junction. (e) Line-height profiles derived from the AFM image of the unannealed junction depicted in (c). The profile in red represents the area of the junction, whereas the profile in black corresponds to a region where the two nanowires do not overlap. (f) Similar to (e) but obtained from the AFM image of the annealed junction depicted in (d).

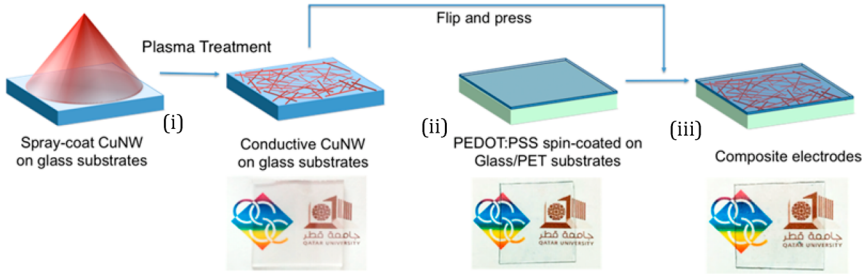

Figure 4. Schematic depiction of the transfer process for spray-coated and plasma-treated CuNWs to a spin-coated PEDOT:PSS film using the "flip and press" method. The photographs below the diagram show, from left to right, (i) CuNWs on a glass substrate, (ii) PEDOT:PSS film on a PET substrate, and (iii) hybrid TCE on a PET substrate. In each case, the OSC and QU logos are placed beneath the substrate in order to allow visual comparison of the various samples' transparencies.

onto a different glass or poly(ethylene terephthalate) (PET) substrate coated with a conductive polymer film (PEDOT:PSS), thus embedding the CuNWs into the conductive polymer and producing a smooth electrode, precisely as reported by Gaynor et al.[16] The schematic of the transfer process is shown Figure 4. At first, CuNWs were spray-coated onto a glass substrate and, subsequently, plasma treated under previously described conditions. Typically, films of plasma-treated CuNWs had T_{550} = 87% and sheet resistance R_s = 23.1 ± 4.8 Ω/sq. As a receiving layer, PEDOT:PSS was spin-coated onto a glass or a PET substrate and dried. Typical PEDOT:PSS thin films used in this work have thickness ∼70 nm. The sheet resistance of the PEDOT:PSS film, being greater than 500 kΩ/sq, is therefore negligible as a contributing factor to the final conductivity of the composite electrode. The preannealed (percolated) CuNW network was finally transferred onto the PEDOT:PSS film under the ∼20 MPa pressure of a shop press. The transfer process has nearly a 100% yield, meaning that all of the nanowires from the donor substrate were transferred to the target substrate (see Figure 3 of the Supporting Information). After a complete transfer, the PET/PEDOT:PSS/CuNW samples had a sheet resistance of R_s ∼ 25Ω/sq, consistent with that of the initial (i.e., bare) CuNW network.

Figures 5a and 5b are the cross-sectional SEM images of the transferred CuNWs on PET substrates without and with the PEDOT:PSS thin film. In the absence of the PEDOT:PSS receiving layer, it is easy to observe nanowires sticking out of the plane of the sample (Figure 5a). In contrast, when CuNWs are transferred onto the PEDOT:PSS layer, the cross-sectional profile becomes cleaner and shows fewer nanowires sticking out of the surface (Figure 5b). The reduction of the surface roughness can also be seen from SEM images taken at a viewing angle of 5° (see Figures 5c and 5d). Whereas in Figure 5c spray-coated CuNWs on a glass substrate can be identified individually, especially at the junctions, a smoother and more homogeneous surface is seen to have been obtained in Figure 5d when the CuNWs are transferred onto a PEDOT:PSS layer on a PET substrate. Furthermore, PEDOT:PSS is widely employed in organic electronics applications as a buffer layer between those of ITO and the active materials in order to improve contact and to facilitate charge injection. Therefore,

DOI: 10.1021/acsami.5b01379
ACS Appl. Mater. Interfaces 2015, 7, 16223−16230

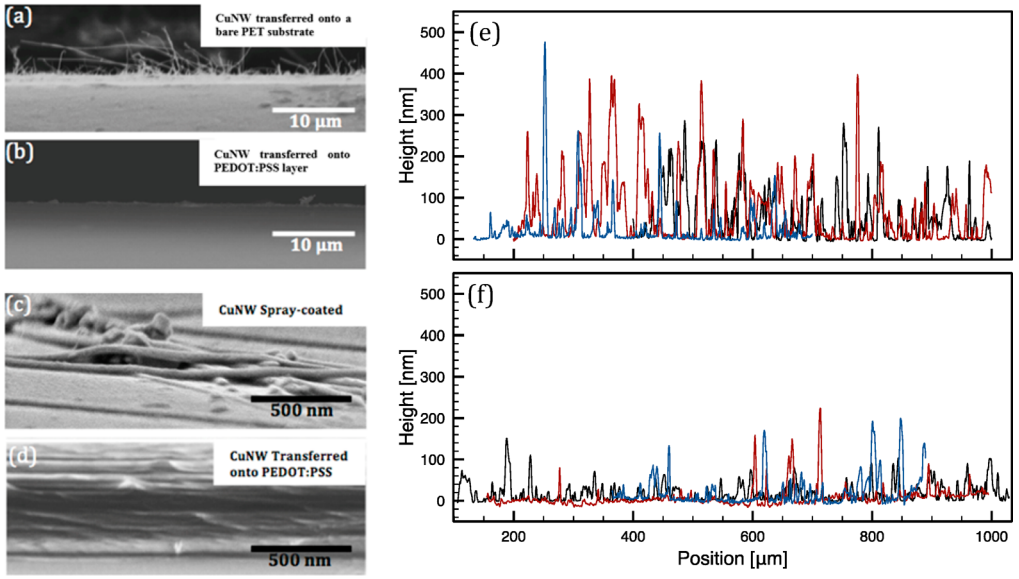

Figure 5. (a) Cross-sectional SEM view of CuNWs transferred to a bare PET substrate, showing numerous nanowires sticking out of the plane of the substrate. (b) Cross-sectional SEM view of CuNWs transferred to a spin-coated PEDOT:PSS film atop a PET substrate; hardly any nanowires are seen to be sticking out of the plane in this case. (c) Angled SEM image of spray-coated CuNWs on a glass substrate. (d) Angled SEM image of CuNWs transferred onto a thin film of PEDOT:PSS atop a PET substrate. (e) Surface profiles of spray-coated CuNWs on a glass substrate; the three scans are shown in different colors. (f) Surface profiles of composite PEDOT:PSS/CuNW thin film exhibiting substantially reduced roughness; different colors represent different scans.

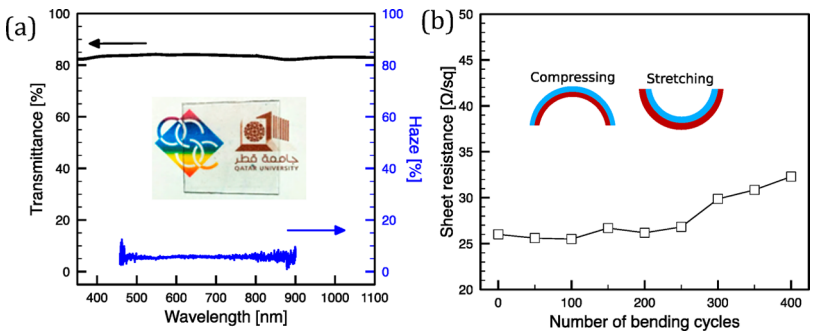

Figure 6. (a) Optical transmittance spectrum (black) and measured haze (blue) of a composite PEDOT:PSS/CuNW sample on a PET substrate. The inset shows a photograph of the corresponding sample placed over OSC and QU logos. (b) Sheet resistance versus the number of bending cycles of a typical composite PEDOT:PSS/CuNW film on PET substrate (bending radius ∼5 cm).

following the lead of Gaynor et al.,[16] we adopted PEDOT:PSS as a receiving layer to improve the smoothness of our CuNW electrodes and also to facilitate integration with active materials for future device explorations.

Using surface profilometry, we measured the surface roughness of our samples; three scanning locations were randomly selected on each sample, and each scan covered the one-millimeter length of a straight line. The results of these measurements are plotted in Figure 5e. Our spray-coated CuNWs on glass (i.e., bare samples) exhibit rough surface profiles, with arithmetic average roughness R_{ave} = 57.28 nm and root-mean-square roughness R_{RMS} = 73.93 nm averaged over the three scans. Many peaks are seen due to the surface morphology of the nanowire network. Figure 5f shows the surface profiles of our PEDOT:PSS/CuNW thin film. A comparison of the height profiles depicted in Figures 5e and 5f reveals a smoother film (i.e., lower peak heights in Figure 5f) for the PEDOT:PSS embedded CuNW networks. The surface roughness values for these films are R_{ave} = 17.4 nm and R_{RMS} = 25.8 nm. Therefore, the transfer of CuNWs into PEDOT:PSS reduces the surface roughness considerably, which is a desirable feature for device integration. Additionally, since the mechanical transfer process does not involve any thermal treatment of the accepting substrate, this technique can be used with different substrate materials, resulting in substrate-independent values of the optical transmittance and of the sheet resistance. The approach, therefore, seems promising for the mass production of high-performance TCEs on flexible, plastic supports.

Our fabricated PEDOT:PSS/CuNW hybrid TCEs, having high optical transmittance and low haze over the visible spectrum (T_{550} = 84.2%; haze ≈ 6% ; see Figure 6a) and also exhibiting low sheet resistance (R_s ∼25Ω/sq), are suitable for many practical applications. To test the mechanical durability of the fabricated TCEs on flexible PET substrates, a sample was bent 400 times (bend radius ∼5 cm), and its sheet resistance was recorded after every 50 bending cycles; the results are plotted in Figure 6b. In the first 300 bending cycles, there was no notable change in R_s, indicating the mechanical stability of

DOI: 10.1021/acsami.5b01379
ACS Appl. Mater. Interfaces 2015, 7, 16223−16230

our composite PET/PEDOT:PSS/CuNW transparent conducting electrodes.

3.3. Composite Electrodes with CuNW/rGO. A major challenge for CuNW films is related to the fact that they oxidize readily, thus decreasing the surface conductivity of the electrode over time. Passivation of these transparent electrodes is therefore critical, even when the TCE is encapsulated within a device, due to the risk of oxidation or impurity diffusion from the active layer. In an attempt to create effective passivation layers, we used pristine graphene platelets as well as reduced graphene oxide (rGO) platelets, using the deposition methods described above. Fabrication of large-area, high-quality graphene sheets using vapor phase methods (as reported in the literature) can be economically prohibitive and requires substantial process optimization, whereas in situ reduction of GO platelets to produce an extremely thin protective layer of graphene over our spray-coated CuNWs is both cost-effective and rapid.

Our GO platelets (purchased from the Graphene Supermarket) have a lateral dimension of ∼5 μm, with 80% of the platelets being in monolayer form. GO platelets were separated from the stock solvent via centrifugation and dispersed in IPA at a concentration of 0.02 mg/mL. Spray-coating this suspension of GO yielded a homogeneous and continuous thin film. Subsequent reduction of GO is necessary for restoring its electrical conductivity.[2,19] After spraying CuNWs and GO (sequentially) on a glass substrate, we annealed the samples in a forming gas environment at 200 °C for 1 h. The reduction of GO could be visually identified by the color change from light brown to black. To further investigate the reduction of GO to rGO, Raman shift was measured on spray-coated GO and rGO thin films (reduced under the aforementioned conditions); the results are presented in Figure 7a. It is seen that the peak of the G band has shifted, upon reduction, from 1598 to 1591 cm^{-1}. The peak intensity ratio between the D band and the G band is also reduced, indicating the partial reduction of GO to rGO.

The SEM image in Figure 7b shows that copper nanowires are covered with a uniform and continuous rGO coating. Small cracks are observed in the SEM image (for instance, within the area marked by a red circle), but overall the nanowires are completely and homogeneously covered by the rGO platelets. The optical transmittance versus sheet resistance of the samples (depicted in Figure 7c) shows that our CuNW films suffer a loss of about ∼4% in transmittance when coated with rGO platelets. Despite the loss of optical transmittance, the sheet resistance as well as the measurement's standard deviation have improved substantially, resulting in a more uniform electrical conductivity across a given sample. In all likelihood, the improvement of conductivity is brought about by the fact that the two-dimensional rGO sheets bridge the gaps between disconnected or nonoverlapping nanowires, thus creating additional pathways for the conduction electrons. Interestingly, if we reverse the order of deposition (that is, spray-coat the substrate with GO platelets first, followed by spray-coating the CuNWs) and anneal the sample under the same conditions as before, we find that the sheet resistance is considerably lowered, while the optical transmittance remains essentially the same as it was when the rGO layer was on top. The samples prepared in the reverse order (i.e., rGO beneath the CuNW layer) show R_s = 5.9 ± 2.1Ω/sq with T_{550} = 83.7%. A SEM image showing such a configuration is shown in Figure 7d.

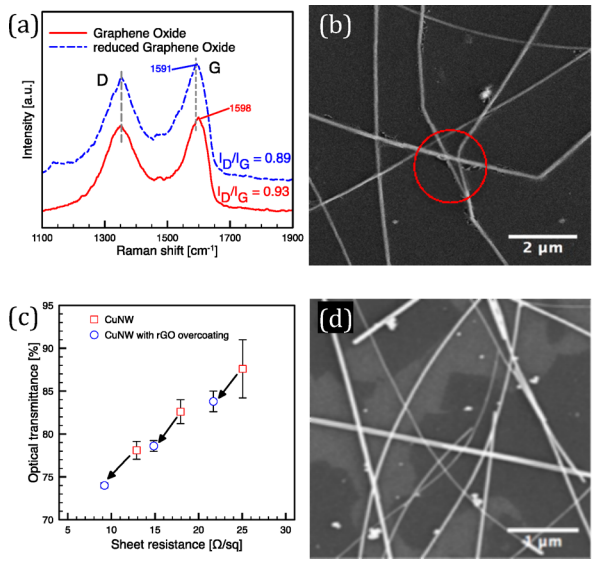

Figure 7. (a) Raman spectroscopy of GO and rGO thin films deposited directly on bare glass substrates. (b) SEM image of CuNWs buried under a homogeneous rGO overcoating; small cracks in the rGO layer are visible within the marked red circle. (c) Optical transmittance at λ = 550 nm versus the sheet resistance of samples of bare CuNW (red) and rGO-covered CuNW (blue), both on glass substrates. (d) SEM image of CuNWs spray-coated over one or more layers of rGO platelets. These reverse-order (i.e., rGO beneath CuNW) electrodes exhibit a remarkable improvement in their sheet resistance with no degradation of their optical transmittance.

We are uncertain as to the cause of this interesting improvement in the electrical conductivity of the samples. It is conceivable that the rGO film makes better contact with CuNWs when the rGO platelets are first deposited on the substrate, since the substrate is much smoother prior to deposition of the CuNW film.

The optical transmittance spectra for bare CuNW films as well as hybrid CuNW/rGO samples are shown in Figure 8a. It is seen that both bare CuNWs and hybrid CuNW/rGO transparent conductive electrodes have fairly flat transmittance over the visible and NIR range. It is also notable that the CuNW/rGO sample has slightly higher haze value (∼6%) than the bare CuNW sample (∼4%).

To test the durability of both CuNW and CuNW/rGO hybrid TCEs, the samples were placed in an enclosed chamber with 80% relative humidity at 80 °C. The sheet resistances were measured every 12 h over 2 days and plotted, as shown in Figure 8b. No change was observed in the optical transmittance of the samples after the exposure. However, the sheet resistance of the bare CuNW TCE is seen to have nearly doubled, while that of the CuNW/rGO hybrid TCE remains essentially intact.

Another durability test was carried out in an ambient environment over a course of 30 days. As seen in Figure 8c, there is an increase of R_s for both CuNW and CuNW/rGO samples during the first 5 days; afterward, while the sheet resistance of the bare CuNW sample continuously increases, the measured R_s of the CuNW/rGO hybrid remains stable over the course of the experiment. These tests highlight the importance of rGO overcoating for the enhanced longevity of our CuNW-based electrodes.

To enable a performance comparison of the various TCEs, the ratio of dc conductivity to optical conductivity is commonly

DOI: 10.1021/acsami.5b01379
ACS Appl. Mater. Interfaces 2015, 7, 16223−16230

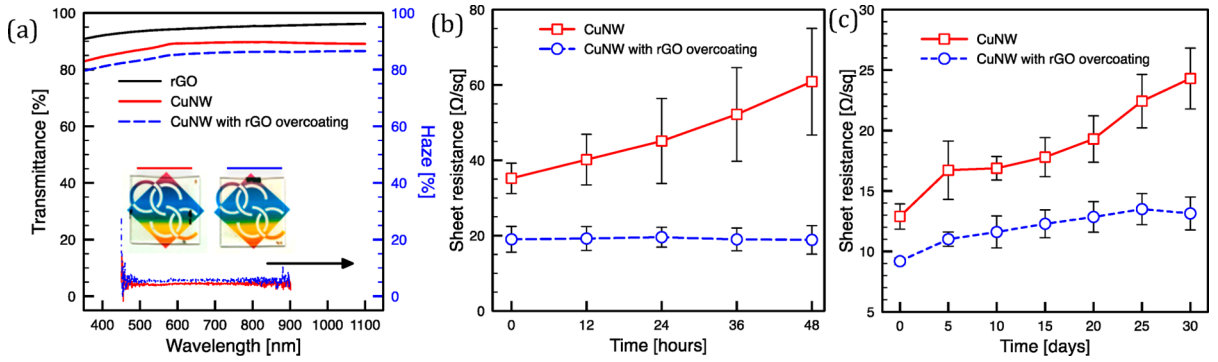

Figure 8. (a) Optical transmittance spectra and haze for an rGO thin-film sample (black), for a bare CuNW film (red), and for a CuNW/rGO hybrid (blue), all on glass substrates. The inset shows photographs of the corresponding samples placed over OSC logos. (b) Durability tests of CuNW (red) and rGO-coated CuNW (blue) TCEs under 80% relative humidity at 80 °C temperature. (c) Durability tests of CuNW (red) and rGO-coated CuNW (blue) TCEs under ambient conditions over the course of 30 days.

used as a key figure of merit (FOM).[20] The following equation relates the transmittance of the film to its sheet resistance:

$$T = \left(1 + \frac{Z_0}{2R_s}\frac{\sigma_{OP}}{\sigma_{dc}}\right)^{-2}$$

Here σ_{OP} and σ_{DC} are the optical and low-frequency (dc) conductivities of the electrode, while $Z_0 \approx 377\ \Omega$ is the impedance of free space. Using the above equation, we computed the ratio σ_{dc}/σ_{OP} and included the values in the summary of our results listed in Table 1. Also, plots of optical transmittance versus sheet resistance for three different values of σ_{dc}/σ_{OP} are included in Figure 9.

Table 1. Performance Evaluation of Our Copper-Nanowire-Based TCEs Compared to Those Reported in the Literature

samples	R_s (Ω/sq)	T_{550} (%)	σ_{dc}/σ_{OP}
CuNW	23.1	87	113
PEDOT:PSS/CuNW	25	84.2	84
CuNW beneath rGO	21.7	83.8	94
CuNW over rGO	5.9	83.7	343
CuNW (ref 15)	51.5	93.1	101
CuNW beneath rGO (ref 19)	34	80	47

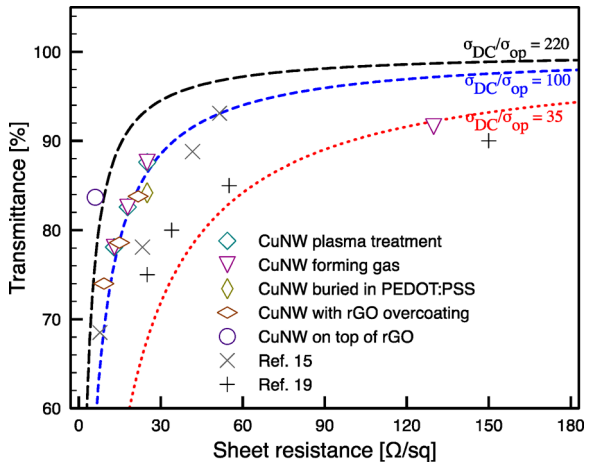

Figure 9. Optical transmittance versus sheet resistance of all TCEs fabricated in the present work. The three dashed lines represent σ_{dc}/σ_{OP} values of 35, 100, and 220, as indicated.

4. CONCLUSIONS

In this work, we have synthesized copper nanowires with ultrahigh aspect ratio ($L/D \approx 1600$) via a solution process and deposited a homogeneous network of these nanowires on glass substrates using a spray-coating technique. Optimal conditions for two annealing methods, thermal annealing and plasma treatment, have been determined for the fabricated CuNW films. The optimized CuNW-based TCEs are subsequently combined with PEDOT:PSS and reduced graphene oxide (rGO) platelets in order to reduce surface roughness and improve durability. Our fabricated TCEs should be suitable for a wide range of optoelectronic applications.

■ ASSOCIATED CONTENT

Supporting Information

SEM images and analysis of dimensions of CuNWs; SEM image showing nanowire deformation after plasma treatment; optical microscope image showing complete transfer of CuNW onto PEDOT:PSS thin film; SEM images showing CuNWs synthesized with the first synthesis method. The Supporting Information is available free of charge on the ACS Publications website at DOI: 10.1021/acsami.5b01379.

■ AUTHOR INFORMATION

Corresponding Authors

*E-mail: zzhu@optics.arizona.edu.
*E-mail: tmankowski@optics.arizona.edu.

Notes

The authors declare no competing financial interest.

■ ACKNOWLEDGMENTS

This publication was made possible by the grant #5-546-2-222 from the Qatar National Research Fund (a member of the Qatar Foundation). The authors also acknowledge partial support from the Arizona TRIF program. The authors are grateful to Professors N. Peyghambarian and R. Norwood for allowing access to their facilities and instrumentation for parts of the work described in this paper. The statements made herein are solely the responsibility of the authors.

■ REFERENCES

(1) Bae, S.; Kim, H.; Lee, Y.; Xu, X.; Park, J.-S.; Zheng, Y.; Balakrishnan, J.; Lei, T.; Kim, H. R.; Song, Y.; Kim, Y.-J.; Kim, K. S.; Özyilmaz, B.; Ahn, J. H.; Hong, B. H.; Iijima, S. Roll-to-Roll

DOI: 10.1021/acsami.5b01379
ACS Appl. Mater. Interfaces 2015, 7, 16223−16230

Production of 30-Inch Graphene Films for Transparent Electrodes. *Nat. Nanotechnol.* **2010**, *5*, 574−578.
(2) Wang, X.; Zhi, L.; Müllen, K. Transparent, Conductive Graphene Electrodes for Dye-Sensitized Solar Cells. *Nano Lett.* **2008**, *8*, 323−327.
(3) Pang, S.; Hernandez, Y.; Feng, X.; Müllen, K. Graphene as Transparent Electrode Material for Organic Electronics. *Adv. Mater.* **2011**, *23* (25), 2779−2795.
(4) Wu, J.; Becerril, H.; Bao, Z.; Liu, Z.; Chen, Y.; Peumans, P. Organic Solar Cells with Solution-Processed Graphene Transparent Electrodes. *Appl. Phys. Lett.* **2008**, *92*, 263302.
(5) Hecht, D. S.; Thomas, D.; Hu, L.; Ladous, C.; Lam, T.; Park, Y.; Irvin, G.; Drzaic, P. Carbon-Nanotube Film on Plastic as Transparent Electrode for Resistive Touch Screens. *J. Soc. Inf. Dispersion* **2009**, *17* (11), 941−946.
(6) Ginley, D. S.; Bright, C. Transparent Conducting Oxides. *MRS Bull.* **2000**, *25* (8), 15−18.
(7) Kim, H.; Horwitz, J. S.; Kushto, G.; Pique, A.; Kafafi, Z. H.; Gilmore, C. M.; Chrisey, D. B. Effect of Film Thickness on the Properties of Indium Tin Oxide Thin Films. *J. Appl. Phys.* **2000**, *88* (10), 6021−6025.
(8) Kim, H.; Horwitz, J. S.; Kushto, G. P.; Kafafi, Z. H.; Chrisey, D. B. Indium Tin Oxide Thin Films Grown on Flexible Plastic Substrates by Pulsed-Laser Deposition for Organic Light-Emitting Diodes. *Appl. Phys. Lett.* **2001**, *79* (3), 284−286.
(9) Saarenpää, H.; Niemi, T.; Tukiainen, A.; Lemmetyinen, H.; Tkachenko, N. Aluminum Doped Zinc Oxide Films Grown by Atomic Layer Deposition for Organic Photovoltaic Devices. *Sol. Energy Mater. Sol. Cells* **2010**, *94* (8), 1379−1383.
(10) Ohyama, M.; Kozuka, H.; Yoko, T. Sol-Gel Preparation of Transparent and Conductive Aluminum-Doped Zinc Oxide Films with Highly Preferential Crystal Orientation. *J. Am. Ceram. Soc.* **1998**, *81*, 1622−1632.
(11) Lee, J.-H.; Park, B.-O. Transparent Conducting ZnO:Al, In, and Sn Thin Films Deposited by the Sol−Gel Method. *Thin Solid Films* **2003**, *426* (1−2), 94−99.
(12) Lee, J.-Y.; Connor, S.; Cui, Y.; Peumans, P. Solution-Processed Metal Nanowire Mesh Transparent Electrodes. *Nano Lett.* **2008**, *8*, 689−692.
(13) Rathmell, A. R.; Bergin, S. M.; Hua, Y. L.; Li, Z. Y.; Wiley, B. J. The Growth Mechanism of Copper Nanowires and Their Properties in Flexible, Transparent Conducting Films. *Adv. Mater.* **2010**, *22* (32), 3558−3563.
(14) Hu, L.; Wu, H.; Cui, Y. Metal Nanogrids, Nanowires, and Nanofibers for Transparent Electrodes. *MRS Bull.* **2011**, *36* (10), 760−765.
(15) Guo, H.; Lin, N.; Chen, Y.; Wang, Z.; Xie, Q.; Zheng, T.; Gao, N.; Li, S.; Kang, J.; Cai, D.; Peng, D.-L. Copper Nanowires as Fully Transparent Conductive Electrodes. *Sci. Rep.* **2013**, *3*, 2323.
(16) Gaynor, W.; Burkhard, G.; McGehee, M.; Peumans, P. Smooth Nanowire/Polymer Composite Transparent Electrodes. *Adv. Mater.* **2011**, *23*, 2905−2910.
(17) Kim, J. Y.; Jung, J. H.; Lee, D. E.; Joo, J. Enhancement of Electrical Conductivity of Poly(3,4-ethylenedioxythiophene)/Poly(4-styrenesulfonate) by a Change of Solvents. *Synth. Met.* **2002**, *126* (2), 311−316.
(18) Gaynor, W.; Lee, J.-Y. Y.; Peumans, P. Fully Solution-Processed Inverted Polymer Solar Cells with Laminated Nanowire Electrodes. *ACS Nano* **2010**, *4*, 30−34.
(19) Kholmanov, I.; Domingues, S.; Chou, H.; Wang, X.; Tan, C.; Kim, J.-Y.; Li, H.; Piner, R.; Zarbin, A.; Ruoff, R. Reduced Graphene Oxide/Copper Nanowire Hybrid Films as High-Performance Transparent Electrodes. *ACS Nano* **2013**, *7*, 1811−1816.
(20) De, S.; Higgins, T. M.; Lyons, P. E.; Doherty, E. M.; Nirmalraj, P. N.; Blau, W. J.; Boland, J. J.; Coleman, J. N. Silver Nanowire Networks as Flexible, Transparent, Conducting Films: Extremely High DC to Optical Conductivity Ratios. *ACS Nano* **2009**, *3*, 1767−1774.

DOI: 10.1021/acsami.5b01379
ACS Appl. Mater. Interfaces 2015, 7, 16223−16230